remote sensing

MDPI

Article

Remote Sensing of Landslide-Generated Sediment Plumes, Peace River, British Columbia

Katie E. Hughes [1,2,*], Amanda Wild [1], Eva Kwoll [1], Marten Geertsema [2], Alexandra Perry [1] and K. Darcy Harrison [1]

[1] Department of Geography, University of Victoria, Victoria, BC V89 5C2, Canada; awild@uvic.ca (A.W.); ekwoll@uvic.ca (E.K.); lperry@uvic.ca (A.P.); k1mb3rly@uvic.ca (K.D.H.)
[2] Ministry of Forests, Lands, Natural Resource Operations and Rural Development, Prince George, BC V2L 1R5, Canada; Marten.Geertsema@gov.bc.ca
* Correspondence: hugheska@uvic.ca

Abstract: Quantifying the contribution of sediment delivered to rivers by landslides is needed to assess a river's sediment load in regions prone to mass wasting. Monitoring such events, however, remains difficult. This study utilised six years of remotely sensed imagery (PlanetScope and RapidEye, Imagery courtesy of Planet Labs, Inc., San Francisco, CA, USA), topographic surveys, and field observation to examine a hydro-geologically controlled, retrogressive landslide near a tributary to the Peace River, British Columbia. The slide has been active since 2014, delivering large amounts of sediment to the Peace River, visible in a persistent plume. Here, we quantify the landslide's sediment contribution to the Peace River, assess the hydro-meteorological drivers of plume variability, and test whether plume activity can be directly linked to landslide activity for monitoring purposes. Our results show that the landslide on average delivered 165,000 tonnes of sediment per year, a seven-fold increase of the tributary's regular load and near half of the Peace River's load at this location. Due to continuous erosion of landslide material, sediment supply is steady and fuelled by repeated failures. Using thresholding, the identification of 'high' plume activity was possible, which positively correlated with the water level in a nearby reservoir, a proxy for the state of groundwater in this region. We reason that 'high' plume activity is linked to increased groundwater pressure because landslide activity is groundwater-controlled and failures fuel sediment delivery to the Peace River. Using readily available imagery, it is thus possible to monitor the activity of this recurrent landslide when field data are difficult to obtain.

Keywords: landslide monitoring; plume detection; PlanetScope; RapidEye; suspended sediment

check for updates

Citation: Hughes, K.E.; Wild, A.; Kwoll, E.; Geertsema, M.; Perry, A.; Harrison, K.D. Remote Sensing of Landslide-Generated Sediment Plumes, Peace River, British Columbia. *Remote Sens.* **2021**, *13*, 4901. https://doi.org/10.3390/rs13234901

Academic Editor: Andrea Ciampalini

Received: 21 October 2021
Accepted: 27 November 2021
Published: 3 December 2021

Publisher's Note: MDPI stays neutral with regard to jurisdictional claims in published maps and institutional affiliations.

Copyright: © 2021 by the authors. Licensee MDPI, Basel, Switzerland. This article is an open access article distributed under the terms and conditions of the Creative Commons Attribution (CC BY) license (https://creativecommons.org/licenses/by/4.0/).

1. Introduction

In regions of river drainage basins highly susceptible to landsliding, strong coupling occurs between the fluvial system and adjacent hillslopes, resulting in the effective delivery and evacuation of large volumes of landslide-derived sediment [1]. Sediment delivery typically occurs episodically, induced by rainfall, snowmelt, earthquakes, or anthropogenic alteration [2] and depends on the characteristics of the landslide, its location in respect to the stream network, and the characteristics of the drainage network [3]. The episodic nature of landsliding renders quantification of its contribution to a river's sediment load difficult and complicates upscaling of local processes for the study of regional landscape evolution [4–6].

Approaches to quantifying sediment delivery by landslides to the river network vary depending on trigger mechanisms identified. In the preparation of sediment budgets, typically only hydroclimatic events are considered, which rely on associating the estimated volume and frequency of past failures with measured precipitation events [7–9]. Other studies have focused on coseismic landslides in steep, mountainous terrain [10,11], where connectivity (and therefore delivery) to the river network is set by drainage density, seismic characteristics, and substrate [3]. However, landslides caused by other trigger mechanisms

and those experiencing multiple or slow failures are commonly overlooked. In Western Canada, recurrent landslides in low-lying terrain that are primarily influenced by fluctuations in groundwater are common [12]. Such landslides may be active for several years and consistently remove sediment from the hillslopes, yet their influence on sediment delivery to river networks has not been investigated.

For a single event, quantification of sediment delivery to the river network is usually performed through analysis of landslide volume (e.g., [13]), direct measurements of suspended sediment concentration at river gauges (e.g., [10,11]), and field surveys of changes in river morphology (e.g., [14]). In the absence of monitoring gauges and in situ observations in remote regions, satellite-based remote sensing technology is utilised to map landslides and identify terrain characteristics (e.g., [15]). The amount of sediment delivered to the river network, however, is not directly quantified by these products. Satellite imagery has previously been used to derive suspended sediment concentrations to study a river's response to flooding and other catchment disturbances (e.g., [16–19]). This method relies on changes in the surface reflectance of water where sediment is present.

Here, we apply calibration to six years of imagery of a sediment-laden plume in the Peace River, British Columbia, generated by a recurrent landslide directly linked to the river network. We use this approach to quantify the variability of sediment delivered to the river by the landslide, investigate whether plume variability is correlated with available hydro-meteorological data, and test whether plume activity can be linked to landslide failure activity for monitoring purposes.

2. Setting

The Peace River lowlands are known to be one of the most landslide-prone areas in Western Canada, with large failures occurring in the Quaternary glaciolacustrine sediments deposited within preglacial valleys [20]. These high-magnitude, low-frequency landslides are well documented [21–24], and influence the Peace River sediment regime, through the development of landslide dams, upstream channel gradient decrease, and affected stream bed armouring [21]. Next to these large failures, recurrent, low-magnitude failures also occur [13,24]. One of these landslides is the Brenot Creek landslide near Hudson's Hope, British Columbia, situated along a tributary of the Peace River.

Since its initiation in 2014, the Brenot Creek landslide has gained regional attention due to a spatially pervasive and persistent sediment plume in the Peace River; a fluvial system of great ecological, cultural, and socio-economic importance in Western Canada [25–27]. Stakeholders fear the adverse impacts associated with persistently high suspended sediment concentrations, specifically the decrease in water quality and the transport of sediment-associated contaminants, such as heavy metals [28,29]. Concentrations of heavy metals (aluminium, arsenic, barium, cadmium, chromium, iron, lead, manganese, and uranium) above the Canadian Water Quality Guidelines were measured at the Peace River confluence immediately following the initial failure [30], upon which water advisories were issued, which continue to remain in place.

The Brenot Creek landslide is located 12 km upstream of the Lynx Creek/Peace River confluence along Brenot Creek, a tributary to Lynx Creek and the Peace River. Originating in the Rocky Mountains, the Peace River is 1923 km long, flows northward to join the Slave and Athabasca Rivers, before eventually draining into the Great Slave Lake and the Arctic Ocean. Since its construction in 1968, the W.A.C. Bennett dam has regulated the Peace River Flow. The dam is located 32 km upstream of the Lynx Creek/Peace River confluence (Figure 1). Under unregulated conditions, peak flows (5510–8810 m^3/s) occurred in late spring and the lowest flows in winter (139–236 m^3/s) (Water Office Canada Station #07EF001). Since regulation, the Peace River usually exhibits low flows during the months of May–July (270–650 m^3/s) and the highest flows in winter (~1500 m^3/s) (ECCC Station #07EF001 [31,32]). The Peace River typically exhibits low amounts of suspended sediment downstream of the W.A.C. Bennet dam (~380,000 tonnes/year) until it reaches

the larger tributaries of Halfway River, Pine River, and Smoky River downstream of the study site [33]. Concentrations are generally coupled to variations in discharge [34].

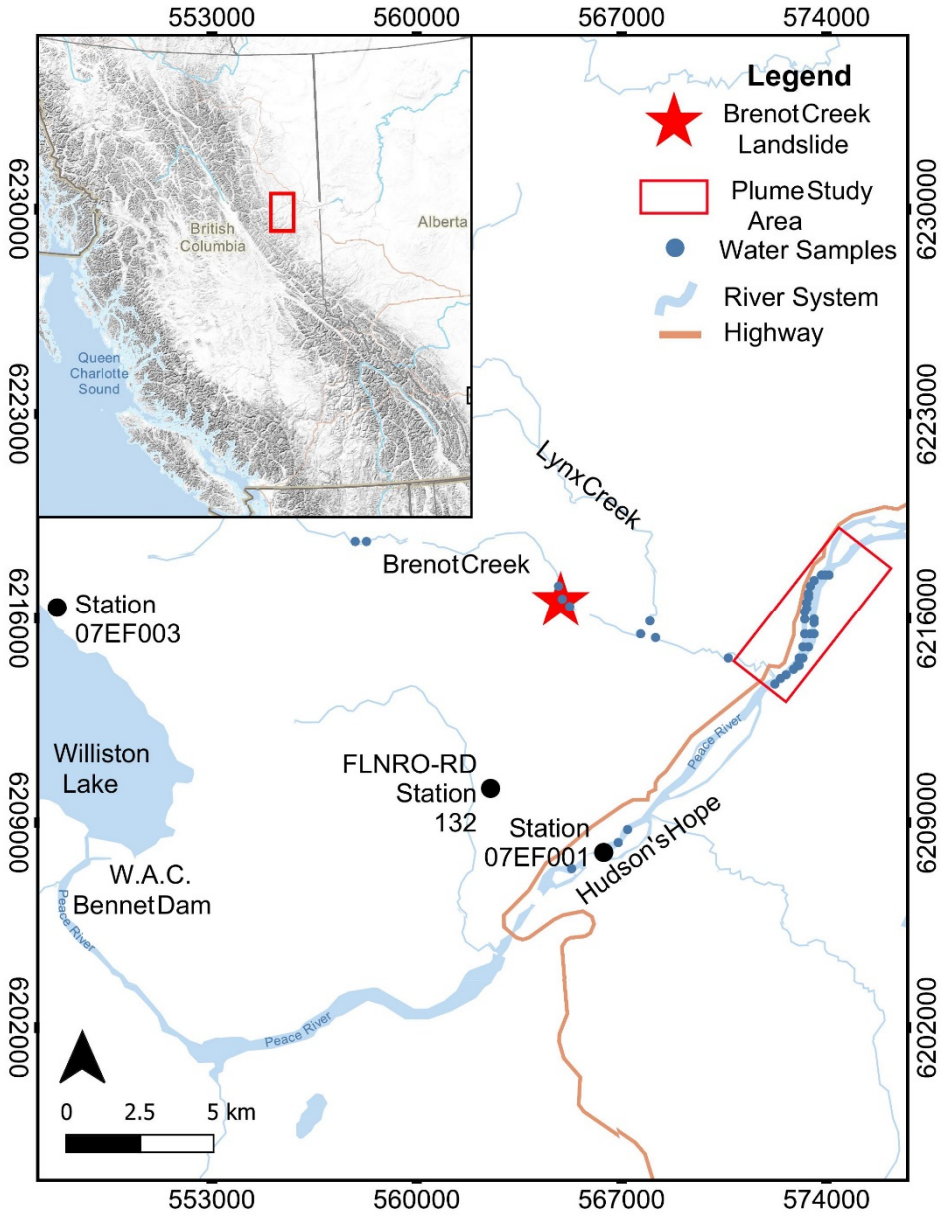

Figure 1. Map of the study area, near Hudson's Hope, British Columbia, Canada. The Brenot Creek Landslide occurs along Brenot Creek, 12 km upstream of the Lynx Creek/Peace River confluence. Plume study area is indicated by a red rectangle downstream of Hudson's Hope with the Peace River flowing to the northeast; also shown are meteorological monitoring stations used in this study and water sampling locations.

The climate of the study area is characterised as a continental subarctic climate with long, cold, and dry winters and short and mild summers. Average temperature ranges from −12.8 °C in January and 16.2 °C in July (WMO Station #71943). Yearly precipitation averages 444.7 mm, forty percent of which occurs as snowfall. Sixty percent of the total precipitation occurs from May to September (WMO Station #71943).

The regional geology is predominantly soft sedimentary bedrock of shale and sandstones of the Fort St. John Group covered with glacial deposits [33,35–37]. Large glacial lakes existed in this area, resulting in thick preglacial deposits of glacial Lake Matthews sediments under the till and post-glacial deposits of glacial Lake Peace above the till [35,36,38].

The layers of clay, silt, sand, and some larger cobbles are typically unconsolidated [37]. Given the surficial and bedrock geology, the area is susceptible to mass wasting events; slides and flows are common in the Peace area [12,24,37]. A documented example is the 1973 Attachie landslide [39,40].

3. Methods

A threefold approach was chosen to quantify the spatial and temporal dynamics of sediment delivery from the Brenot Creek Landslide to the Peace River system: (1) Development and implementation of optical satellite remote-sensing methods to derive the spatial extent, timing, and concentration of incoming landslide sediments into the Peace River; (2) in situ water sampling and monitoring of the landslide, Brenot Creek, and Lynx Creek, to quantify the dynamics of sediment transport through the tributary reaches; (3) statistical analysis of the available proxies for hydrological and meteorological conditions and correlation to temporal patterns in plume activity (derived from the remote sensing analysis) and known slope failures (motion-triggered camera observations).

3.1. Remote Sensing Analysis of Sediment Plume

3.1.1. Calibration Data

In situ water sampling was conducted on 23 May 2018, on the Peace River at the confluence with Lynx Creek to develop suspended sediment concentration calibrations for remotely sensed imagery. Surface water samples (29 total) were collected downstream of the confluence on Peace River both within and outside of the visible sediment plume. The samples were collected in wide-mouth polyethylene sampling bottles and 500 mL samples were filtered using vacuum filtration. This volume was chosen to accommodate the range of concentrations expected for the plume and creek measurements. Sample filters were dried at approximately 105 °C prior to measurement as per the procedure outlined in [41]. Dried samples were then weighted to the nearest 0.1 mg to determine sediment concentration.

3.1.2. Optical Imagery Processing

Suitable RapidEye imagery with 5 m spatial resolution was acquired from September 2014 to November 2016 and PlanetScope imagery with 3 m spatial resolution was acquired from January 2017 to May 2020 courtesy of Planet Labs, Inc. Conditions for retrieval were cloud cover less than 20% and full coverage of the defined river extent (rectangle in Figure 1). Imagery obtained within the same week was analysed only if the plume visually differed in size and shape. With these specifications, 69 satellite images were used in the analysis. Due to a high prevalence of snow and cloud cover, images from the months November, December, and January were difficult to obtain.

Pre-processing of imagery included atmospheric correction (RapidEye only), image normalisation, and sub-setting imagery to a constant extent for the comparison of plume width and concentration within the area directly near the Lynx Creek and Peace River confluence (rectangle in Figure 1). Atmospheric correction was applied via ATCOR in PCI's Geomatica for the purpose of deriving surface reflectance from total reflectance, accounting for sun and sensor angles, adjacency effects, and atmospheric conditions. PlanetScope imagery is received as a surface reflectance product radiometrically corrected using calibration targets. All imagery was spectrally normalised against the 19 May 2018 image, the closest suitable image to the date of field sampling, via relative normalisation of pseudo-invariant features (PIFs). There was no precipitation between imagery date and sample date; however, changes in hydrological conditions may have occurred and introduced potential error. Relative normalisation is a common approach for similar studies of aquatic remote sensing [42]. The PIFs used were clear deep water and exposed sand, which represent the spectral endmembers and are the most applicable for aquatic remote sensing [43]. The spectral signature of each PIF was extracted across all images and plotted against the PIF spectra obtained from the 19 May 2018 imagery via linear regression. The R^2 for all

available bands (blue to NIR) in all images compared to the 19 May 2018 spectra fell within the 0.90–0.99 range. The regression equations obtained were then applied to each spectral band. The output of spectral normalisation is consistent reflectance values, which allows for temporal image-to-image comparison.

3.1.3. Quantification of Suspended Sediment Concentration

Spectral signatures for each in situ water sample location were extracted from PlanetScope and RapidEye imagery. The spectral reflectance value (refVal) for red, red edge (RapidEye only), and near-infrared (NIR) bands and sediment concentration (mg/L) from all 29 Peace River water samples were used to produce a calibration linear regression. The spectral composition was chosen based on known optical properties. Sediment scatters and reflects NIR energy, whilst water strongly absorbs NIR energy [44]. Reflection in the red spectrum stabilises due to saturation in high total suspended sediment conditions [44]. A multi-band approach was found to improve the performance of plume categorisation in multiple preliminary trials compared to a single-band approach. The inclusion of the red edge for RapidEye imagery also increased the equation performance.

The derived equations (Equation (1) for PlanetScope and (2) for RapidEye) were then applied to each pixel across every image collected between 2014 and 2020 to estimate sediment concentration based on the spectral reflectance of the satellite imagery. The linear regressions using the spectra and water sample concentrations resulted in a coefficient of determination (R^2) of 0.59 and 0.52 for Equation (1) (Planetscope) and Equation (2) (RapidEye), respectively.

$$\text{Concentration } = 0.2199 * \frac{\text{red refVal } + \text{NIR refVal}}{2} - 127.41 \quad (1)$$

$$\text{Concentration } = 17.605 * \frac{\text{red refVal } + \text{NIR refVal} + \text{Red Edge refVal}}{3} - 70.17 \quad (2)$$

This range of R^2 values reflects, within the Peace River, a change in spectral reflectance was not always matched with a change in concentration. Spectral reflectance in the water column within red and NIR bands may also vary in the presence of organic material [45], which was not assessed in this study. The suspended sediment concentration may have also changed between the date of image acquisition (19 May 2018) and the date of water sampling (23 May 2019). However, the R^2 values for both PlanetScope and RapidEye are within typical ranges (0.5 to 0.8) of values obtained in similar studies [44,46,47].

After the spectral pixels were converted into concentrations, for each image a sediment concentration raster was exported to GIS. This was then classified to differentiate between sediment and water, with eight levels of suspended sediment concentration. Binary classification (plume/no plume) was also conducted to produce plume vectors and calculate plume extent. After classifications were complete, the plume extent, mean concentration, and maximum and minimum concentrations were calculated to provide insight into the temporal and spatial variance of the plume.

3.2. Field Observation of Slide Activity and Sediment Transport in Brenot Creek and Lynx Creek

3.2.1. Slide Mechanisms and Failure Activity

The landslide was visited on multiple occasions to qualitatively describe slide headwall characteristics, failure mechanisms, and landslide activity. Light Detection and Ranging (LiDAR) data from August 2006 (Airborne Imaging Inc. commissioned by FLNRO-RD using the Optech 3100 Lidar system) was compared against digital elevation models (DEMs) derived from structure-from-motion (SfM) using images collected during drone flights in October 2014, October 2015, and July 2017 to assess the volume of displaced material during the initial failure as well as headwall characteristics. A motion-triggered wildlife camera was installed facing the slide and provided imagery between August and November 2016. The images were used to visually determine the date of large failure events during this period.

3.2.2. Sediment Transport in Brenot Creek and Lynx Creek

To understand the processes of sediment transport occurring prior to the delivery of landslide sediment to the Peace River, eight transects were collected from Lynx and Brenot Creeks on 22 & 24 May 2018 to determine channel width, depth, velocity, and sediment concentration (Figure 1). Velocity was measured with a Sontek Flowtracker flow meter. At three locations across the channel, equally spaced proportional to the total channel width, velocity measurements were taken across creek transects at 20% and 80% of the water depth and only at 60% of the water depth when the water was shallow (under 0.6 m) [48]. Pebbles, boulders, and shallow water in Brenot Creek locations near the slide resulted in negative velocity measurements, due to turbulence, and failed to calculate discharge and sediment load in the creek directly at the slide site. The sediment concentration was determined by collecting eight additional water samples at the same depth and location as the flow tracker and following the same filtering protocol as the river plume filters [41]. Discharge was calculated using the channel depth, width, and velocity. Where discharge was available, the suspended sediment load was calculated through multiplication with the average sediment concentration from all samples collected in that transect.

3.3. Analysis of Plume Activity in Hydro-Climatic Context

3.3.1. Hydro-Climatic Data

Hydrological and meteorological data from secondary sources were obtained to understand the factors influencing the pattern in sediment delivery from the Brenot Creek Landslide to the Peace River. Daily data for temperature and precipitation were obtained from the BC Ministry of Forests, Lands, Natural Resource Operations, and Rural Development (FLNRO-RD) Wildfire Service weather station network, Station 132 (location shown in Figure 1). Daily discharge for the Peace River at Hudson's Hope was obtained from Water Office Canada Station 07EF001 (location shown in Figure 1). The station was discontinued in 2019. Since discharge in the Peace River is regulated by the W.A.C. dam, the amount of added water from the surrounding area, such as spring snowmelt, surface flow, and groundwater infiltration, was assessed via measurements of the daily water level of Williston Lake (W.A.C. reservoir, location shown in Figure 1). This value can also inform groundwater conditions, as there is no publicly available data on groundwater in the study area. This is substantiated through a report by BCOGRIS [32], which noted a link between the Williston Lake water levels and the groundwater flow, postulating that water follows the pre-glacial valley from the reservoir and flows on the silt/clay lacustrine deposit. Williston Lake water level data were obtained from Water Office Canada Station 07EF003 (location shown in Figure 1).

3.3.2. Spearman's and Kendall Correlation

Using these daily data, the following variables were then correlated against the remotely sensed plume characteristics (mean plume concentration, plume area, the product of concentration and area, and mean plume concentration grouped into low, moderate, and high): discharge (m^3/s), water level at Williston Reservoir (m), precipitation (mm), temperature (°C), and discharge (weekly average) (m^3/s). To account for potential lags, the plume characteristics were also correlated against metrics including the seven days prior to the image acquisition date. This includes water level (weekly average) (m), precipitation (weekly sum) (mm), and temperature (weekly range) (°C). Given the discrete and stochastic nature of the landslide activity and the irregular time interval of the satellite imagery, time series analysis could not be accomplished. Instead, Spearman's and Kendall correlations were applied, using paired values by date. The application of these correlation tests was selected based on the non-parametric nature, the application of the underlying assumptions to our study design, as well as their frequent usage in hydro-climatic data analysis [49–51]. The environmental conditions and plume characteristics were also compared to known

failure dates identified from the motion-triggered wildlife camera installed at Brenot Creek Landslide.

4. Results

4.1. The Brenot Creek Landslide

The initial failure of the Brenot Creek Landslide occurred in early September 2014, enlarging the zone of depletion from its pre-2014 state. The initial inspection revealed that a historic landslide zone of depletion was reactivated, developing a fresh scarp in pre- and post-glacial glaciolacustrine sands and silts (Figure 2a,c). The slide affected an area of 9500 m^2, with a 50-m-high head scarp exposing horizontally bedded glacial sediment. Field observations of the slide over the study period from September 2014 to May 2020 indicated that the landslide was intermittently failing throughout this period, depositing silt and sand into Brenot Creek and the connected fluvial system. Based on surface differencing of the available DEMs of the landslide site, approximately 540,000 m^3 of sediment was evacuated from the scar area from 2014 to 2020 (Table 1). The initial failure exposed the groundwater table at the base of the slope, in which an unnamed stream began to flow, continuously saturating the colluvial sand and silt deposited by cliff collapse on the landslide floor (Figure 2b). The continued flow of groundwater following the initial failure is indicative of high pore-water pressure at the base of the slide and thus likely contributed to the initial failure and the ongoing instability of the area. Toe erosion from piping and seepage collapsed the cliff face, causing a retrogressive headward migration of the scarp. Additional material then fell from the cliff, forming colluvial aprons. These became saturated, flowed away from the scarp for a minor distance, and accumulated in a thick deposit below the main scarp. With continued retrogressive backweathering and oversteepening, episodic substantial cliff collapses of dry sand and silt continued to fall on the original mass, and through undrained loading [52], resulting in another large rapid flow. A cyclic failure dynamic persisted over the study period, which manifests in the sporadic occurrence of landslide dams in Brenot Creek (Figure 2c), the filling of Lynx Creek with thick sediment, and dissemination of sediment-laden water within the Peace River.

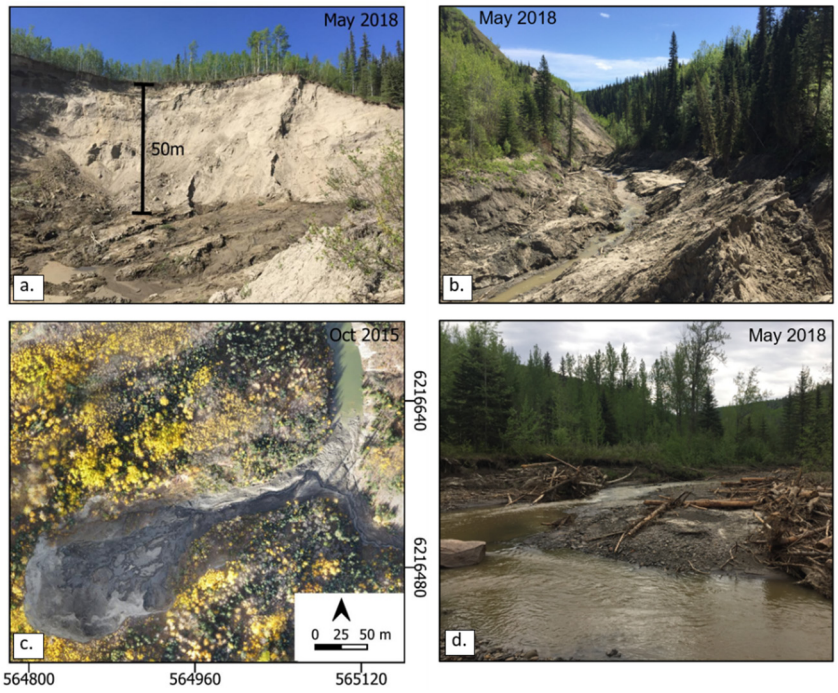

Figure 2. Overview of the Brenot Creek Landslide. (**a**) Landslide scar in 2018, (**b**) Brenot Creek downstream of the landslide in 2018, (**c**) aerial drone orthomosaic imagery of the landslide scar in 2015 showing temporary landslide dam, and (**d**) Lynx Creek in 2018. Woody debris and coarser riverbed sediment can be found on bars along the channel.

Table 1. Changes to landslide scar dimensions measured from DEMs of the study site (2006, 2014, 2015, 2017). The deficit volume implies the minimum volume of sediment lost from the scarp area over the stated time period. This change does not take into account the sediment accumulating in the bowl between major flushes resulting from large cliff collapses.

Survey Dates Compared	Change in Width (m)	Headwall Retreat (m)	Sediment Lost from Landslide (m^3)
2016 vs. 2014 (Initial Failure)	28	4	99,000
2014 vs. 2015	2	22	75,000
2015 vs. 2017	33	63	265,000
2017 to 2020	8	31	102,000 [1]
Net Change	71	120	541,000

[1] Volume estimated from regression of dimension changes and volume change from previous years.

Along Brenot Creek and Lynx Creek, deposits of landslide material and uprooted trees are found along the banks and in the form of in-channel deposits (Figure 2b). This material is generally finer than the creek's bed material, which consists of gravel and sand mixtures (Figure 2d).

Visual inspection of the available (August–November, 2016) motion-triggered wildlife camera showed nine visible events when large portions of the creek bed and surrounding area were flooded with sediment from the slope. The events varied in size with smaller failures often occurring 2–3 days prior to bigger events.

4.2. Temporal and Spatial Plume Dynamics

A total of 69 satellite images were analysed from September 2014 to May 2020. The maximum plume extent within the analysis window occurred on 26 April 2017 (931,995 m^2), and the minimum on 5 December 2018 (no detectable plume) (Figure 3). On average, the plume extent was 412,400 m^2, although it illustrated a high level of spatial variability over time, with a standard deviation of 248,977 m^2. The highest average concentration occurred on 8 February 2020, and the lowest occurred on 5 December 2018, when the plume was not detectable (Figure 3). The mean concentration was 69 mg/L. Plume 'magnitude' (the product of area and mean concentration) peaked on 26 April 2017 and was the lowest on 5 December 2018. It should be noted that plume concentration and plume area are only weakly positively correlated.

The average plume concentration was further used to classify images into low, moderate, and high plume activity: Low plume activity assumes the plume concentration is between 0 and 30 mg/L, an upper limit that is roughly two times the background turbidity observed directly upstream of the Lynx Creek confluence (an average suspended sediment concentration of 14.9 mg/L obtained from repeated measurement between 2010 and 2011 [53]). Moderate plume activity denotes concentrations between two to four times the background suspended sediment concentration (30 mg/L to 120 mg/L) and high plume activity exceeding four times the background suspended sediment concentration (>120 mg/L). Low plume activity (below 30 mg/L) occurs in 20% of the imagery used, moderate plume activity (30–120 mg/L) for 64% of the imagery used, and high plume activity (>120 mg/L) for 16% of the imagery used. Figure 4 illustrates the temporal distribution of plume concentration and activity by month.

It is evident from remote-sensing analysis that the plume activity is stochastic, lacking a significant seasonal or temporal trend. Overall, the months of June and July show low–moderate plume activity with little variability, while high activity occurs during January–May only (with the exception of the year 2019). This is also the period where activity is the most varied throughout the years. Variability appears to increase slightly after July, while overall concentrations remain moderate.

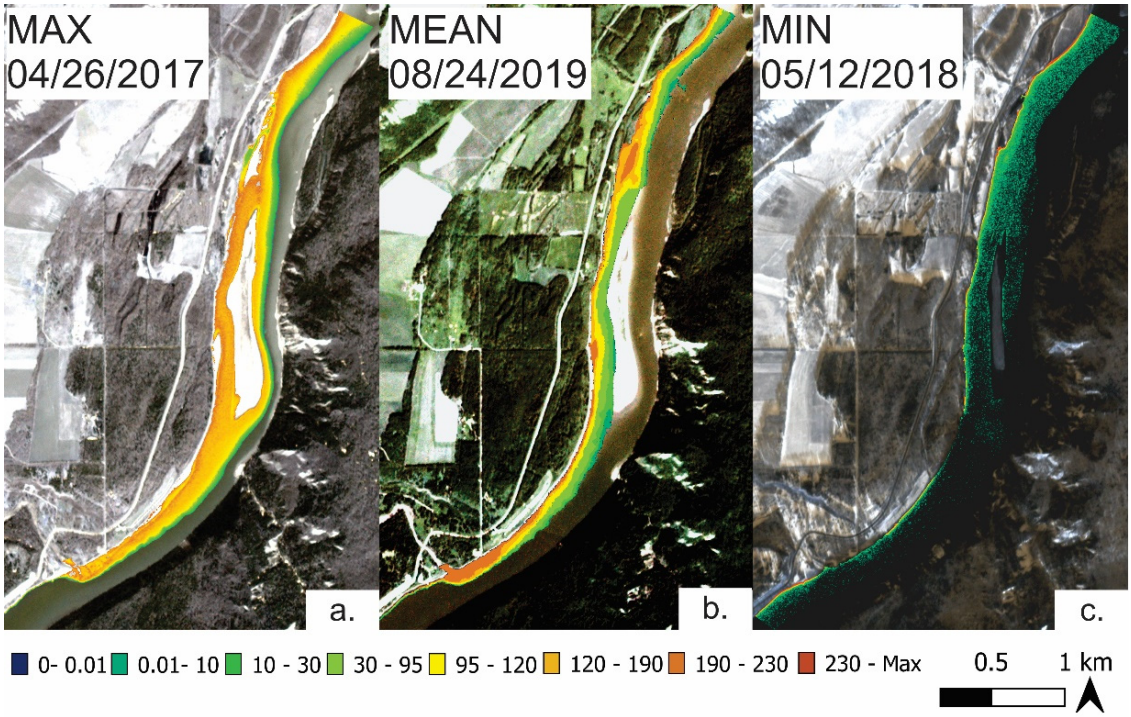

Figure 3. Suspended sediment concentration (mg/L) during (**a**) maximum, (**b**) mean, and (**c**) minimum plume magnitude (the product of plume area and mean concentration). Imagery courtesy of Planet Labs, Inc.

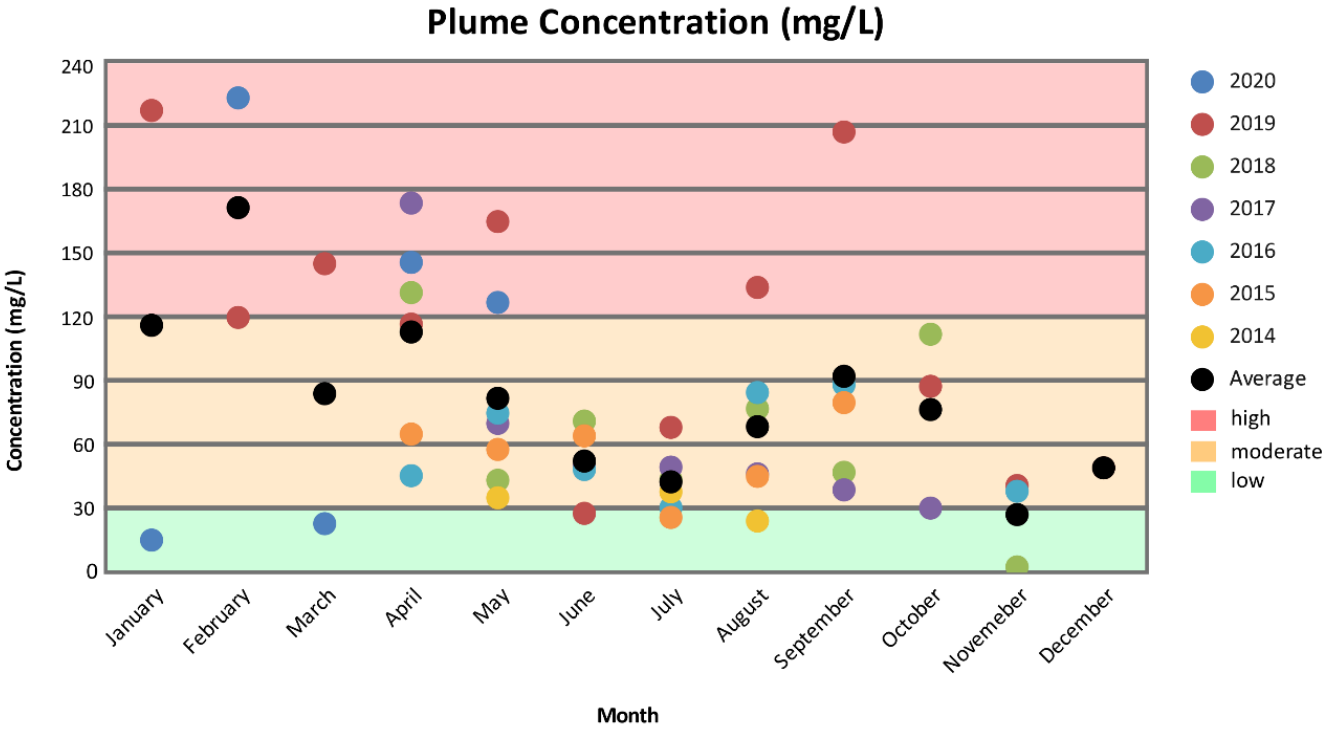

Figure 4. Suspended sediment concentration in the Peace River plume (mg/L) by month from 2014 to 2020 obtained via satellite imagery analysis. Plume activity is indicated by colour shading (see text for explanation).

4.3. Brenot Creek and Lynx Creek Sediment

The average sediment concentration derived during water sampling on 22–24 May 2018 directly below the Brenot Creek Landslide was recorded at 16,276 mg/L, while directly upstream of the slide the average concentration was 121 mg/L (Figure 5). The unnamed

muddy creek leaving the slide towards Brenot Creek had a concentration of 151,615 mg/L. Lynx Creek, prior to the confluence with Brenot Creek, had a concentration of 117 mg/L, while Brenot Creek, just above the confluence with Lynx Creek, still had a concentration of 12,699 mg/L. After the confluence of the two creeks but prior to reaching the Peace River, the sediment concentration of Lynx Creek was measured at 1470 mg/L (Figure 5). Estimated sediment loads are available for Brenot and Lynx Creeks upstream of the Brenot/Lynx confluence (1.96 kg/s and 0.05 kg/s, respectively), immediately downstream of the confluence (2.31 kg/s), and near the Lynx/Peace confluence (0.86 kg/s). For reference, the mean plume concentration on 23 May 2018 during this period was calculated at 34.28 mg/L with an extent of 477,792 m^2. This falls in the moderate activity category.

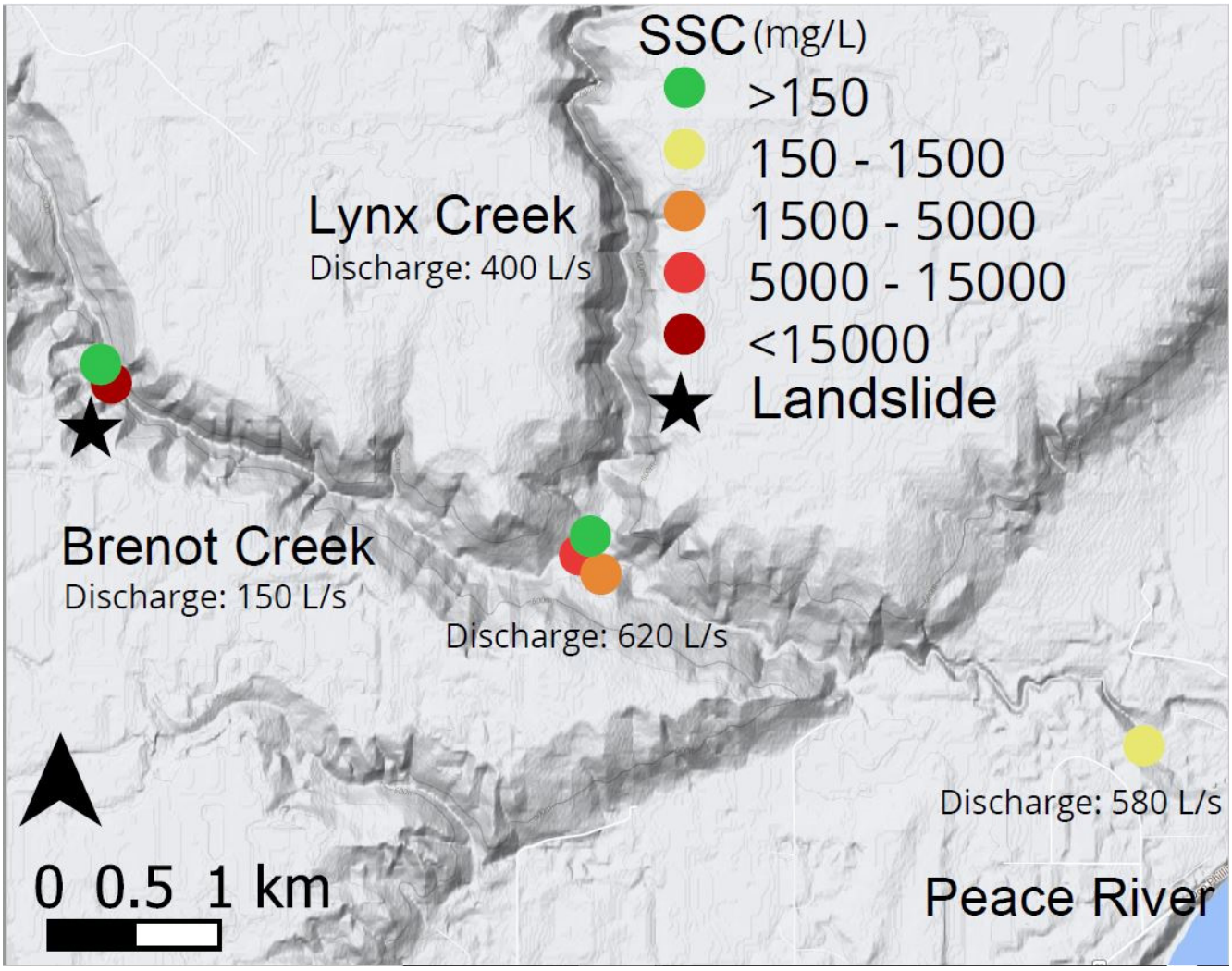

Figure 5. Suspended sediment concentration (SSC) for Brenot Creek and Lynx Creek tributaries, 22–24 May 2018.

4.4. Hydrological and Meteorological Control on Plume Variability

The series of correlation analyses undertaken on the full dataset of imagery showed only one significant correlation (>±0.5) of the hydrological or meteorological variables included in this study (Figure 6). This correlation is between discharge and the plume area and is moderately inversely correlated (−0.58 (Spearman's (S)) to −0.42 (Kendall (K))). This suggests that large discharges from the Peace River cause the incoming sediment-laden water from the Lynx Creek tributary to be constrained to the western bank. When plume data are grouped by low, moderate, and high concentration, 'high' plume activity is moderately positively correlated to the reservoir water level of Williston Reservoir

(0.55 (K), 0.67 (S)), and moderately positively correlated to the weekly average water level of Williston Reservoir (0.64 (K), 0.78 (S)). 'Low' plume activity was moderately positively correlated to temperature (0.45 (K), 0.56 (S)). It should be noted the confidence in these correlations is lowered by the smaller sample sizes (N = 11 for high, N = 14 for low activity) of grouped data. Furthermore, there appears to be no relationship between temperature or precipitation events and failures captured in the period of observation from the motion-triggered camera. Events occurred in the temperature ranges of −1 °C to 12 °C, both with and without the occurrence of precipitation events.

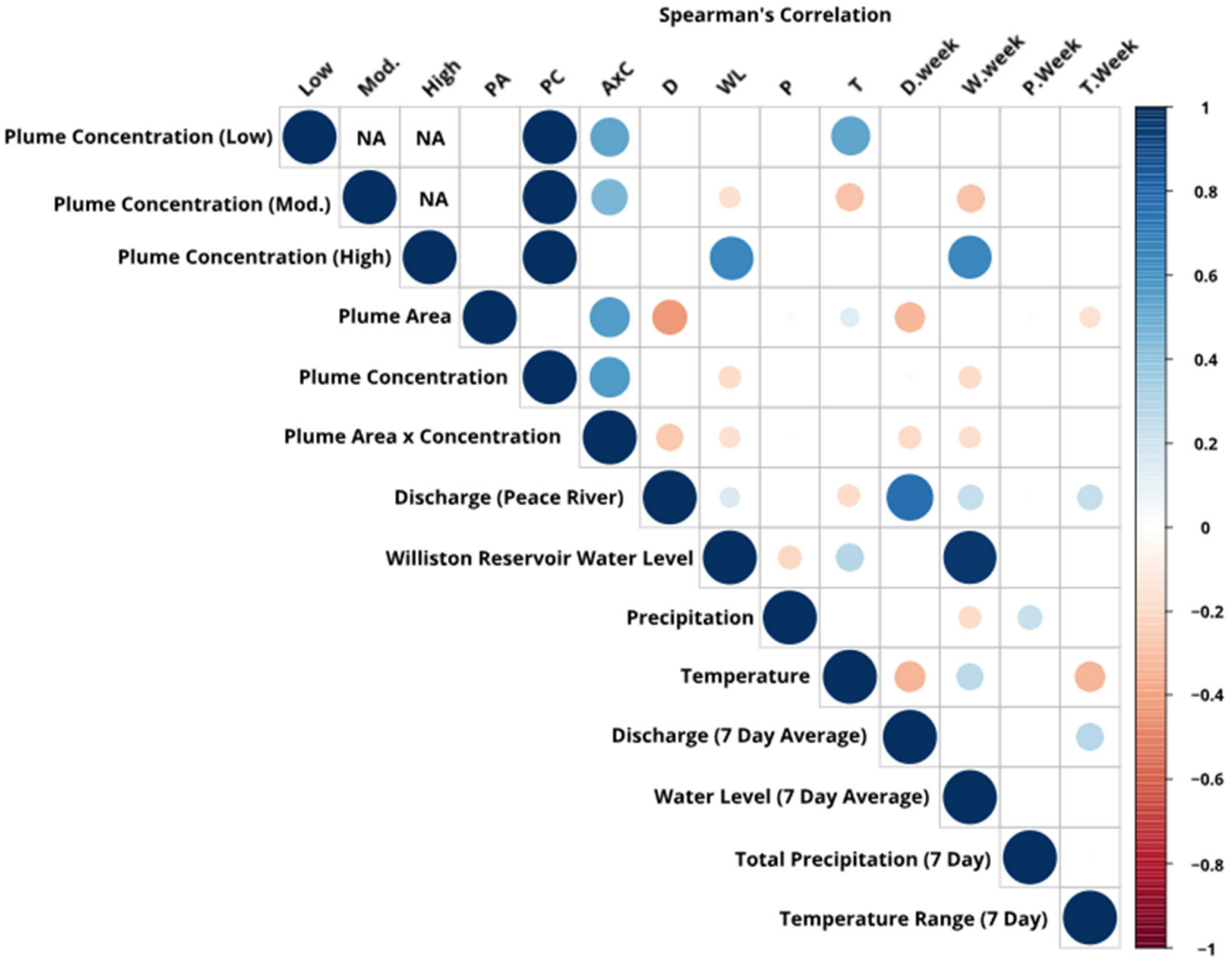

Figure 6. Correlation plot for hydro-meteorological variables and plume concentrations using Spearman's correlation with a significance value of 0.1. The diameter of circles, as well as colour scale, indicate the strength of correlation.

5. Linking Remotely Sensed Plume Concentrations to Landslide Activity

The magnitude and speed of sediment delivery from a landslide to the adjacent fluvial system depend on the variability of the supply of sediment from the landslide and the speed of sediment evacuation, and hence the overall connectivity within the fluvial network [54,55]. Our observations suggest that sediment delivery from the Brenot Creek Landslide to the Peace River is variable and only partially linked to the failure activity at the slide itself. One reason for this is that due to the presence of a newly formed stream exiting the failing slope of the Brenot Creek Landslide, the sediment supply to the Peace River tributaries is ongoing and fuelled by the continued slow erosion of material deposited during failure events at the foot slope. Supply may be interrupted only due to the temporary formation of landslide dams during slope failure. While supply is continuous, connectivity varies throughout the observation period and depends on the

transport capacity and competency of Brenot Creek and Lynx Creek. In the following, we distinguish three different levels of plume activity (low, moderate, and high) and link them to sediment delivery mechanisms from the landslide to Peace River.

During periods of 'low' plume activity, low discharge of tributary streams reduces the capacity of the system to evacuate sediments, causing little to no connectivity of the landslide to the fluvial system. These conditions were observed during the winter and summer months but were not found during transitional months (April/May and September/October). Transport-limited conditions in the predominantly groundwater-sourced Brenot Creek and Lynx Creek [32] may occur for several reasons: due to a landslide dam blocking the creek, due to partial freeze-over under cold temperatures, and due to a decrease in groundwater flow and/or increased evaporation under warmer temperatures. The correlation analysis depicted a positive correlation between the plume concentration and temperature under 'low' activity, indicating that the amount of sediment delivered to the Peace River is higher (though overall 'low') during these periods in the summer compared to the winter, likely due to the partial freeze-over. The absence of 'low'-activity periods in transitional months is likely due to the creeks never being transport-limited, causing connectivity and plume activity to be at least 'moderate'.

Periods of 'moderate' plume activity are marked by the consistent delivery of fine sediments from the landslide to the Peace River resulting in 'moderate' plume concentrations. These periods occurred most often and were observed throughout the year, with plume concentrations (though 'moderate') being generally lower in June/July and November/December than during other months of the year. Fluctuations in tributary discharge during these periods may be caused by local precipitation, increased evaporation, or variability in groundwater flow. No significant correlation was found between the hydrological and meteorological variables and plume concentration during these periods, indicating that none of them stand out as driving variables. Field observations at the landslide site during one of these periods (May 2018) indicated no presence of landslide activity and considerable erosion of the fine landslide sediments by the groundwater seepage from the landslide face. Though supply is continuous, temporary storage and resuspension along the tributary may further introduce variability in plume activity. Our limited observations on sediment concentrations in the stream indicate sediment deposition along the tributaries towards the Peace River, confirmed by deposits of finer, landslide-sourced sediment over the coarser Brenot Creek and Lynx Creek gravel/sand mixture.

Periods of 'high' plume activity are not dictated solely by an increased fluvial transport capacity, but rather by events of increased sediment supply due to slope failures or landslide dam breakage. 'High'-activity periods were observed predominately from January to May, though events occur in August and September of 2019 as well. No 'high' activity was noted during June/July and November/December in any of the years. The positive correlation of Williston dam water levels (a proxy for changes in aquifer conditions [32]) to plume concentrations at 'high' plume activity, could point to increased instability of the Brenot Creek Landslide with increased pore water pressure due to changes in the hydraulic head [56]. Increased groundwater flow would exacerbate the cyclical nature of the failure. By proxy of failure mechanism, landslide activity increases both the fluvial transport capacity, through the increased exposure of the aquifer, and the supply of fine sediments. The failure activity causes regression of the slope face, therefore causing heightened seepage of groundwater, acting as a built-in mechanism for delivery to the fluvial system. The absence of 'high'-activity periods detected during the months of June/July is likely a result of lower groundwater levels, absence of failures, and reduced overall flow, the latter of which also caused an overall lower delivery to the Peace River during 'moderate' periods. 'High'-activity periods are also absent in November/December, which next to an overall lack of data could be the result of frozen grounds and partially frozen creeks.

Linking landslide activity to plume dynamics for monitoring purposes is complex. Using thresholding of average plume concentrations, as performed here, as a proxy for monitoring recurrent failure of the landslide is possible. The thresholds chosen in this

work warrant further validation via direct slope observation. Overall, 11 'high'-activity events were identified over the years, some years saw no or only one event (2014, 2015, 2017, 2018), and some years were particularly active (2019 and 2020). It is clear, however, that the Peace River is impacted throughout the year even when large catastrophic failures are absent. High-resolution optical remote sensing of water bodies is a frequently used monitoring technique for water quality applications [57,58]. Our research shows that the expansion of such monitoring approaches to recurrent landslides is promising, though it cannot succeed without knowledge of the landslide mechanics, the hydrological system, and connectivity therein. The approach could be improved by direct measurement of fluctuations in groundwater conditions and a longer motion-triggered camera observation campaign to further our understanding of the failure mechanisms and the drivers of high sediment plume activity.

6. Impact of the Recurrent Landslide on the Fluvial System

Over the six-year study period, no evidence (from remote sensing analysis and field observations) suggested the landslide was stabilising. Analysis of aerial imagery and LiDAR data suggests headwall retreat and lateral retreat are persistent (Table 1). Additionally, the number of occurrences of 'high' and 'moderate' plume activity was greater in 2019 and 2020 compared to 2015 and 2016, resulting in overall higher average plume concentrations across all images (49 mg/L, 53 mg/L, 84 mg/L, and 102 mg/L for 2015, 2016, 2019, and 2020, respectively). The impact of this landslide on the fluvial system is thus long-lived. The contributions of landslides are often overlooked in general sediment budgeting, despite observations that sub-catchments with landslides covering 1% of the area can provide 65% of the total sediment flux [1]. When landslides are considered, it is the contributions of large-volume, low-frequency events that are taken into account [21,23,59]. Our observations show that the sediment contribution of recurrent low-magnitude, but high-frequency landslides are significant; prior to the landslide, from 2000 to 2010, Lynx Creek had an average yearly suspended sediment load of 23,400 tonnes/year [53]. Surface differencing of DEMs collected from 2014 to 2020 showed, on average, 165,000 tonnes/year are delivered from the Brenot Creek Landslide to the fluvial system, which will, over time, arrive at the Peace River.

The additional sediment may cause aggregation and degradation along the course of the Peace River, though no studies are available yet. It may change the composition of the riverbed and alter the characteristics of bedforms, similar to previous observations of analogous events [60]. Such sedimentological changes adversely affect river habitats [61]. In addition, the sediment delivered contains naturally occurring contaminants, which are dispersed through the fluvial system causing the degradation of water quality. Water testing indicated contaminated levels exceeding the Canadian Water Quality Guidelines (drinking water and freshwater aquatic life) at sites directly downstream of the Brenot Creek Landslide, the Lynx Creek confluence, and the Peace River confluence [30]. Even after stabilisation, contaminant levels may remain high for some time until all deposits are eroded [62].

An examination of drone imagery flown in August 2006 around Lynx Creek and Brenot Creek (Airborne Imaging Inc. commissioned by FLNRO-RD) shows geomorphological evidence of older scars of rotational landslides in the area immediately surrounding the Brenot Creek Landslide and a shift to complex earthflows in the north (Figure 7). Further study is required to elucidate why this shift occurs and is out of the scope of this study. This finding suggests that the impact of recurrent, low-magnitude landslides in this region reaches far beyond the Brenot Creek Landslide, and the Peace River may have frequently been affected by similar events in the past.

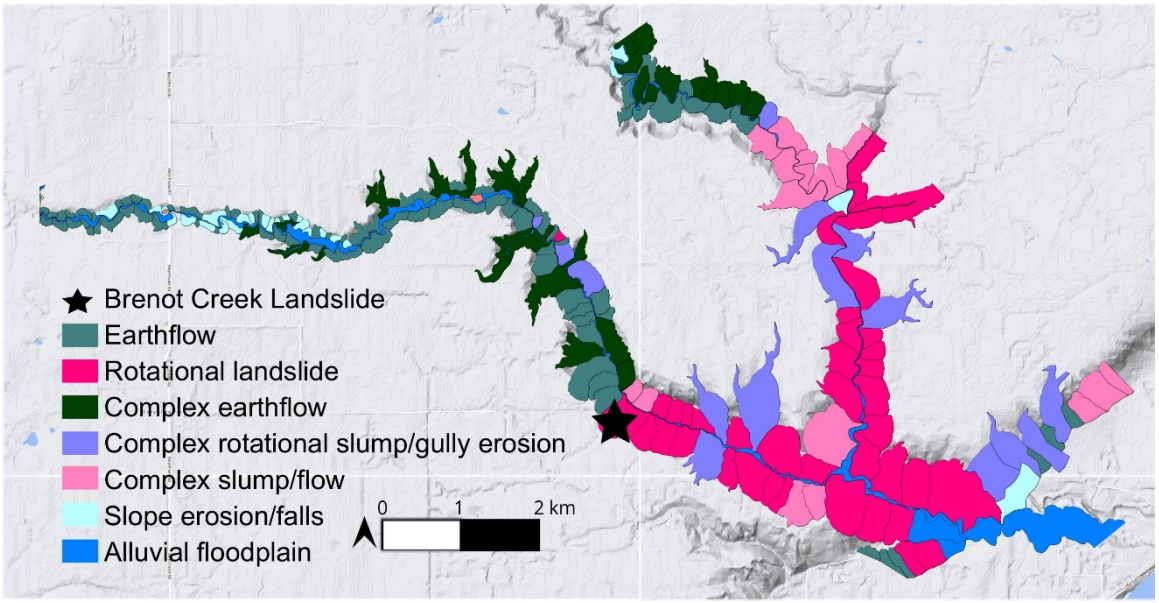

Figure 7. Geomorphically annotated LiDAR for the Lynx Creek and Brenot Creek Tributaries depicting the pervasive nature of various landslide scars. Rotation landslides, such as the Brenot Creek Landslide are shown in magenta.

7. Future of the Landslide and Plume

Further understanding of the precise details of the drivers of failure is necessary to predict when the landslide will stabilise. The literature suggests that the onset of landslide stabilisation and the beginning of system recovery will be dependent on the geological nature of the area [60,63]. The Deforest Creek Slide, WA, analogous in regard to failure mechanisms (retrogressive landslide with hydrogeological triggers), stabilised only when the head escarpment made contact with a sandstone geological unit with greater stability following eight years of activity [60]. Stabilisation could also occur when the landslide becomes disconnected from the water table (naturally or through intervention), which would consequently reduce the connectivity of the slide to the wider fluvial system [63,64]. It is expected that the Peace River plume would cease exhibiting high concentrations as a result of stabilisation but continue exhibiting moderate plume concentrations until all landslide-sourced material is evacuated.

8. Conclusions

This study utilised six years of remotely sensed imagery, topographic data, and field observations to study the Brenot Creek Landslide and the spatio-temporal variability of its landslide-generated sediment plume in the Peace River, British Columbia. Rapid Eye and Planetscope spectral reflectance were calibrated towards suspended sediment concentration using in situ water samples. Velocity, turbidity measurements, and water samples were collected along the tributaries from the landslide to Peace River. Repeat high-resolution DEMs from LiDAR and SfM imagery were collected. The results shed light not only on the nature of the contribution of sediment to the Peace River by the low-magnitude recurrent landslide, but also on the suitability of the remote sensing approach for monitoring landslide activity. Our conclusions are as follows:

- The sediment plume is persistent, fluctuates in concentration throughout the year, and shows no evidence of ceasing. At the same time, headwall retreat and the removal of mass at the groundwater-controlled slide are ongoing.
- Surface differencing of DEMs yielded an upper estimate of sediment delivery to the Peace River of 165,000 tonnes/year, significantly higher than the pure riverine load of 23,400 tonnes/year [60]. Topographic evidence of similar geomorphic features in the

nearby area suggests that low-magnitude, recurrent landslides play a significant role in the sediment delivery of the Peace River catchment.

- The link between plume concentration and landslide activity is complex. The continuous erosion of landslide deposits by the ever-flowing tributaries results in steady delivery to the Peace River, resulting in plume sediment concentrations with temporal variability throughout the year.
- Low plume concentrations occur in either the winter months, when the creeks are partially frozen or in the summer months, possibly linked to a decrease in the groundwater-sourced discharge.
- Moderate plume concentrations occur during all months of the year, though concentrations tend to be lower among the moderately ranging events in the summer.
- High plume concentration does not occur during the summer months and is positively correlated to water level at a nearby reservoir—a proxy for overall groundwater conditions at the site. We interpret this as evidence that high plume concentrations may be linked to the failure of the groundwater-controlled landslide or the removal of a large amount of material from the landslide site.
- Only high plume concentrations are therefore immediately linked to failure. Further validation is required to determine whether our plume activity threshold (<120 mg/L) is suitable. Using said threshold, monitoring of landslide activity in the coming years via remote sensing is possible.
- Application of this concept to other recurrent landslides that are immediately linked to a river network is possible when the hydro-climatic context is sufficiently known.

Author Contributions: Methodology, A.W., K.E.H., E.K. and M.G.; formal analysis, K.E.H., A.W. and K.D.H.; fieldwork and data collection, E.K., M.G., A.W., A.P. and K.D.H.; data curation, A.W., K.E.H. and K.D.H.; writing, K.E.H. and E.K.; writing—review and editing, E.K., K.E.H., A.W., M.G., K.D.H. and A.P.; visualization, K.E.H. and A.P.; supervision, E.K. and M.G.; project administration, M.G. and E.K.; funding acquisition, M.G. and E.K. All authors have read and agreed to the published version of the manuscript.

Funding: Funding was provided to E.K. and M.G. via FLNRO-RD research funds.

Institutional Review Board Statement: Not applicable.

Informed Consent Statement: Not applicable.

Data Availability Statement: E.K. and M.G. were given access to Planet labs imagery via academic licenses. Data available on request.

Acknowledgments: We thank past Hudson Hope's Mayor Gwen Johansson and Leigh Summers for background information and logistical support, and James Jacklin for his review of the work. We would like to acknowledge the School of Geography, Environment, and Earth Sciences, Victoria University of Wellington, New Zealand and Helmholtz-Zentrum Potsdam, Deutsches GeoForschungsZentrum for where K. Hughes and A. Wild are now currently affiliated, respectively. However, contributions to this research were completed prior at the University of Victoria, Geomorphology of Coastal Systems lab.

Conflicts of Interest: The authors declare no conflict of interest.

References

1. Clapuyt, F.; Vanacker, V.; Christl, M.; Van Oost, K.; Schlunegger, F. Spatio-temporal dynamics of sediment transfer systems in landslide-prone Alpine catchments. *Solid Earth* **2019**, *10*, 1489–1503. [CrossRef]
2. Dethier, E.; Magilligan, F.J.; Renshaw, C.E.; Nislow, K.H. The role of chronic and episodic disturbances on channel–hillslope coupling: The persistence and legacy of extreme floods. *Earth Surf. Process. Landf.* **2016**, *41*, 1437–1447. [CrossRef]
3. Li, G.; West, A.J.; Densmore, A.L.; Hammond, D.E.; Jin, Z.; Zhang, F.; Wang, J.; Hilton, R.G. Connectivity of earthquake-triggered landslides with the fluvial network: Implications for landslide sediment transport after the 2008 Wenchuan earthquake. *J. Geophys. Res. Earth Surf.* **2016**, *121*, 703–724. [CrossRef]

4. Swanson, F.J.; Fredriksen, R.L. Sediment routing and budgets: Implications for judging impacts of forestry practices. In *Sediment Budgets and Routing in Forested Drainage Basins*; Swanson, F.J., Janda, R.J., Dunne, T., Swanston, D.N., Eds.; U.S. Department of Agriculture, Forest Service, Pacific Northwest Forest and Range Experiment Station: Portland, OR, USA, 1982; pp. 129–137.
5. Campforts, B.; Shobe, C.M.; Steer, P.; Vanmaercke, M.; Lague, D.; Braun, J. HyLands 1.0: A hybrid landscape evolution model to simulate the impact of landslides and landslide-derived sediment on landscape evolution. *Geosci. Model Dev.* **2020**, *13*, 3863–3886. [CrossRef]
6. Broeckx, J.; Rossi, M.; Lijnen, K.; Campforts, B.; Poesen, J.; Vanmaercke, M. Landslide mobilization rates: A global analysis and model. *Earth Sci. Rev.* **2020**, *201*, 102972. [CrossRef]
7. Reid, L.M.; Dunne, T. Sediment budgets as an organizing framework in fluvial geomorphology. In *Tools in Fluvial Geomorphology*; Wiley: Hoboken, NJ, USA, 2016; pp. 357–380.
8. Ibsen, M.-L.; Brunsden, D. The nature, use and problems of historical archives for the temporal occurrence of landslides, with specific reference to the south coast of Britain, Ventnor, Isle of Wight. *Geomorphology* **1996**, *15*, 241–258. [CrossRef]
9. Korup, O. Large landslides and their effect on sediment flux in South Westland, New Zealand. *Earth Surf. Process. Landf.* **2005**, *30*, 305–323. [CrossRef]
10. Lin, G.-W.; Chen, H.; Hovius, N.; Horng, M.-J.; Dadson, S.; Meunier, P.; Lines, M. Effects of earthquake and cyclone sequencing on landsliding and fluvial sediment transfer in a mountain catchment. *Earth Surf. Process. Landf.* **2008**, *33*, 1354–1373. [CrossRef]
11. Hovius, N.; Stark, C.P.; Hao-Tsu, C.; Jiun-Chuan, L. Supply and Removal of Sediment in a Landslide-Dominated Mountain Belt: Central Range, Taiwan. *J. Geol.* **2000**, *108*, 73–89. [CrossRef]
12. Geertsema, M.; Clague, J.J.; Schwab, J.W.; Evans, S.G. An overview of recent large catastrophic landslides in northern British Columbia, Canada. *Eng. Geol.* **2006**, *83*, 120–143. [CrossRef]
13. Fuller, I.C.; Riedler, R.A.; Bell, R.; Marden, M.; Glade, T. Landslide-driven erosion and slope-channel coupling in steep, forested terrain, Ruahine Ranges, New Zealand, 1946–2011. *Catena* **2016**, *142*, 252–268. [CrossRef]
14. Kasai, M.; Brierley, G.; Page, M.; Marutani, T.; Trustrum, N. Impacts of land use change on patterns of sediment flux in Weraamaia catchment, New Zealand. *Catena* **2005**, *64*, 27–60. [CrossRef]
15. Metternicht, G.; Hurni, L.; Gogu, R. Remote sensing of landslides: An analysis of the potential contribution to geo-spatial systems for hazard assessment in mountainous environments. *Remote Sens. Environ.* **2005**, *98*, 284–303. [CrossRef]
16. Mertes, L.A.K.; Smith, M.O.; Adams, J.B. Estimating suspended sediment concentrations in surface waters of the Amazon River wetlands from Landsat images. *Remote Sens. Environ.* **1993**, *43*, 281–301. [CrossRef]
17. Wang, J.J.; Lu, X.X. Estimation of suspended sediment concentrations using Terra MODIS: An example from the Lower Yangtze River, China. *Sci. Total Environ.* **2010**, *408*, 1131–1138. [CrossRef]
18. Pavelsky, T.M.; Smith, L.C. Remote sensing of suspended sediment concentration, flow velocity, and lake recharge in the Peace-Athabasca Delta, Canada. *Water Resour. Res.* **2009**, *45*, 11. [CrossRef]
19. Bonansea, M.; Fernandez, R.L. Remote sensing of suspended solids concentration in a reservoir with frequent wildland fires on its watershed. *Water Sci. Technol.* **2013**, *67*, 217–223. [CrossRef] [PubMed]
20. Davies, M.; Paulen, R.; Hickin, A. *Inventory of Holocene Landslides, Peace River Area, Alberta (NTS 84C)*; Alberta Energy and Utilities Board: Edmonton, AB, Canada, 2005.
21. Miller, B.G.N. Two Landslides and Their Dams, Peace River Lowlands. Master's Thesis, University of Alberta, Edmonton, AB, Canada, 2000.
22. Miller, B.; Dufresne, A.; Geertsema, M.; Atkinson, N.; Evensen, H.; Cruden, D. Longevity of dams from landslides with sub-channel rupture surfaces, Peace River region, Canada. *Geoenviron. Disasters* **2018**, *5*, 1. [CrossRef]
23. Kim, T.H.; Cruden, D.M.; Martin, C.D.; Froese, C.R. The 2007 Fox Creek landslide, Peace River Lowland, Alberta, Canada. *Landslides* **2010**, *7*, 89–98. [CrossRef]
24. Severin, J.M. Landslides in the Charlie Lake Map Sheet, Fort St. John. Ph.D. Thesis, University of British Columbia, Vancouver, BC, Canada, 2004.
25. Loo, T. Disturbing the Peace: Environmental Change and the Scales of Justice on a Northern River. *Environ. Hist.* **2007**, *12*, 895–919. [CrossRef]
26. Waite, J.; Gruber, H. Peace River Site C Project: Environmental Studies; Development of a Mitigation AND Compensation Program; and Project Licencing. *Can. Water Resour. J.* **1981**, *6*, 20–37. [CrossRef]
27. Canadian Environmental Assessment Agency; BC Hydro. *Report of the Joint Review Panel: Site C Clean Energy Project*; B.C. Hydro and Power Authority, British Columbia, under the Authority of the Federal Minister of the Environment, Gov-ernment of Canada: Ottawa, ON, Canada; B.C. Minister of Environment, Government of British Columbia: Victoria, BC, Canada, 2014; ISBN 978-1-100-23631-5.
28. Peraza-Castro, M.; Sauvage, S.; Sánchez-Pérez, J.M.; Ruiz-Romera, E. Effect of flood events on transport of suspended sediments, organic matter and particulate metals in a forest watershed in the Basque Country (Northern Spain). *Sci. Total Environ.* **2016**, *569*, 784–797. [CrossRef]
29. Quinton, J.N.; Catt, J.A. Enrichment of Heavy Metals in Sediment Resulting from Soil Erosion on Agricultural Fields. *Environ. Sci. Technol.* **2007**, *41*, 3495–3500. [CrossRef] [PubMed]

30. District of Hudson's Hope; Ministry of Forests, Lands, Natural Resource Operations; Rural Development, BC; Northern Health, BC; Ministry of Health, BC. *Lynx Creek/Brenot Creek Water Quality Testing [Digital Data]*; District of Hudson's Hope: Prince George, BC, Canada, November 2014.
31. Butcher, G.A. *Peace River Area: Peace River Mainstem Water Quality Assessment and Objectives*; Water Quality Unit, Resource Quality Section, Water Management Branch: Victoria, BC, Canada, 1987.
32. Ortman, B.; Diversified Technical Services; BC OGRIS. Groundwater Monitoring in the Greater Hudson Hope Area (Final Report). 2005. Available online: http://www.bcogris.ca/documents/scek/Final_Reports/d-ECIM-Com-DTS-2004-21-Rep.pdf (accessed on 21 March 2021).
33. Church, M. *The Regulation of Peace River: A Case Study for River Management*; Wiley: Hoboken, NJ, USA, 2014.
34. Church, M. Geomorphic response to river flow regulation: Case studies and time-scales. *Regul. Rivers Res. Manag.* **1995**, *11*, 3–22. [CrossRef]
35. Mathews, W.H. *Quaternary Stratigraphy and Geomorphology of Charlie Lake (94A) Map-Area, British Columbia*; Canadian Geological Survey: Ottawa, ON, Canada, 1978. [CrossRef]
36. Hartman, G.; Clague, J. Quaternary stratigraphy and glacial history of the Peace River valley, northeast British Columbia. *Can. J. Earth Sci.* **2008**, *45*, 549–564. [CrossRef]
37. Van Esch, K.J.B. Failure Behaviour of Bedrock and Overburden Landslides of the Peace River Valley near Fort St. John, British Columbia. Ph.D. Thesis, University of British Columbia, Vancouver, BC, Canada, 2012.
38. Hickin, A.S.; Lian, O.B.; Levson, V.M.; Cui, Y. Pattern and chronology of glacial Lake Peace shorelines and implications for isostacy and ice-sheet configuration in northeastern British Columbia, Canada. *Boreas* **2015**, *44*, 288–304. [CrossRef]
39. Evans, S.G.; Hu, X.Q.; Enegren, E.G. The 1973 Attachie slide, Peace River valley, near Fort St. John, B.C., Canada: A landslide with a high-velocity flow slide component in Pleistocene sediment. In Proceedings of the 7th International Symposium on Landslides, Balkema, Trondheim, Norway, 17–21 June 1996; pp. 715–720.
40. Fletcher, L.A. Failure Behaviour of two Landslides in Silt and Clay. Ph.D. Thesis, University of British Columbia, Vancouver, BC, Canada, 2000.
41. Multi Agency Laboratory Analytical Protocols (EPA). Chapter 12: Laboratory Sample Preparation, EPA 402-B-04-001B. 2004. Available online: https://www.epa.gov/sites/production/files/2015-05/documents/402-b-04-001b-12-final.pdf (accessed on 21 May 2018).
42. Olthof, I.; Pouliot, D.; Fernandes, R.; Latifovic, R. Landsat-7 ETM+ radiometric normalization comparison for northern mapping applications. *Remote Sens. Environ.* **2005**, *95*, 388–398. [CrossRef]
43. Rowlands, G.P.; Purkis, S.J.; Riegl, B.M. The 2005 coral-bleaching event Roatan (Honduras): Use of pseudo invariant features (PIFs) in satellite assessments. *J. Spat. Sci.* **2008**, *53*, 99–112. [CrossRef]
44. Wang, C.; Chen, S.; Li, D.; Wang, D.; Liu, W.; Yang, J. A Landsat-based model for retrieving total suspended solids concentration of estuaries and coasts in China. *Geosci. Model Dev.* **2017**, *10*, 4347–4365. [CrossRef]
45. Ruddick, K.G.; De Cauwer, V.; Park, Y.-J.; Moore, G. Seaborne measurements of near infrared water-leaving reflectance: The similarity spectrum for turbid waters. *Limnol. Oceanogr.* **2006**, *51*, 1167–1179. [CrossRef]
46. Zhan, C.; Yu, J.; Wang, Q.; Li, Y.; Zhou, D.; Xing, Q.; Chu, X. Remote sensing retrieval of surface suspended sediment concentration in the Yellow River Estuary. *Chin. Geogr. Sci.* **2017**, *27*, 934–947. [CrossRef]
47. Pereira, F.J.S.; Costa, C.A.G.; Foerster, S.; Brosinsky, A.; de Araújo, J.C. Estimation of suspended sediment concentration in an intermittent river using multi-temporal high-resolution satellite imagery. *Int. J. Appl. Earth Obs. Geoinf.* **2019**, *79*, 153–161. [CrossRef]
48. Michaud, J.P.; Wierenga, M. Estimating Discharge and StreamFlows: A Guide for Sand and Gravel Operators. *Ecol. Publ.* **2005**, *70*, 37.
49. Hamed, K.H. Trend detection in hydrologic data: The Mann–Kendall trend test under the scaling hypothesis. *J. Hydrol.* **2008**, *349*, 350–363. [CrossRef]
50. Hamed, K.H. The distribution of Spearman's rho trend statistic for persistent hydrologic data. *Hydrol. Sci. J.* **2016**, *61*, 214–223. [CrossRef]
51. Liang, L.; Li, L.; Liu, Q. Precipitation variability in Northeast China from 1961 to 2008. *J. Hydrol.* **2011**, *404*, 67–76. [CrossRef]
52. Hutchinson, J.N.; Bhandari, R.K. Undrained loading, a fundamental mechanism of mudflows and other mass movements. *Geotechnique* **1971**, *21*, 353–358. [CrossRef]
53. Canadian Environmental Assessment Agency; BC Hydro; Golder Associates. Site C Clean Energy Project: Baseline Aquatic Productivity in the Upper Peace River; 2012; Volume 2, Appendix P. Available online: https://iaac-aeic.gc.ca/050/documents_staticpost/63919/85328/Vol2_Appendix_P.pdf (accessed on 12 September 2020).
54. Imaizumi, F.; Sidle, R.C. Linkage of sediment supply and transport processes in Miyagawa Dam catchment, Japan. *J. Geophys. Res. Earth Surf.* **2007**, *112*, F3. [CrossRef]
55. Cavalli, M.; Trevisani, S.; Comiti, F.; Marchi, L. Geomorphometric assessment of spatial sediment connectivity in small Alpine catchments. *Geomorphology* **2013**, *188*, 31–41. [CrossRef]
56. Abramson, L.W. *Slope Stability and Stabilization Methods*; Wiley: New York, NY, USA, 1996.
57. Ritchie, J.; Zimba, P.; Everitt, J. Remote Sensing Techniques to Assess Water Quality. *Photogramm. Eng. Remote Sens.* **2003**, *69*, 695–704. [CrossRef]

58. Brando, V.E.; Dekker, A.G. Satellite hyperspectral remote sensing for estimating estuarine and coastal water quality. *IEEE Trans. Geosci. Remote Sens.* **2003**, *41*, 1378–1387. [CrossRef]
59. Morgan, A.J.; Paulen, R.C.; Slattery, S.R.; Froese, C.R.; Energy Resources Conservation Board. *Geological Setting for Large Landslides at the Town of Peace River, Alberta (NTS 84C)*; Alberta Geological Survey: Edmonton, AB, Canada, 2012.
60. Thompson, J.N. The Deforest Creek Landslide and Sediment Transport in Deer Creek, Skagit County, Washington. Master's Thesis, Western Washington University, Bellingham, WA, USA, 1988. [CrossRef]
61. Kemp, P.; Sear, D.; Collins, A.; Naden, P.; Jones, I. The impacts of fine sediment on riverine fish. *Hydrol. Process.* **2011**, *25*, 1800–1821. [CrossRef]
62. Göransson, G.; Norrman, J.; Larson, M. Contaminated landslide runout deposits in rivers—Method for estimating long-term ecological risks. *Sci. Total Environ.* **2018**, *642*, 553–566. [CrossRef] [PubMed]
63. Cavers, D.S. Groundwater blow off & piping debris-flow failures. In Proceedings of the 3rd Canadian Conference on Geotechnique & Natural Hazards, Edmonton, AB, Canada, 9–10 June 2003; pp. 151–158.
64. Geertsema, M.; Schwab, J.W.; Jordan, P.; Millard, T.H.; Rollerson, T.P. Hillslope processes. In *Compendium of Forest Hydrology and Geomorphology in British Columbia, BC Ministry of Forest and Range*; Pike, R.G., Redding, T.E., Moore, R.D., Winker, R.D., Bladon, K.D., Eds.; Province of British Columbia: Victoria, BC, Canada, 2010; Volume 66, pp. 213–273.